DOI: 10.4274/tjo.galenos.2022.23855
Turk J Ophthalmol 2023;53:37-43

Original Article

# Artifact-Removed Quantitative Analysis of Choriocapillaris Flow Voids

M. Giray Ersöz*, Mümin Hocaoğlu**, Işıl Sayman Muslubaş**, Serra Arf**, Erdost Yıldız***, Murat Karaçorlu**

*Biruni University Faculty of Medicine, Department of Ophthalmology, İstanbul, Türkiye
**İstanbul Retina Institute, İstanbul, Türkiye
***Koç University Faculty of Medicine, Translational Medicine Application and Research Center, İstanbul, Türkiye

## Abstract

**Objectives:** To investigate choriocapillaris flow voids (FV) with a new optical coherence tomography angiography (OCTA) image processing strategy that can eliminate artifacts caused by vitreous opacities, sub-retinal pigment epithelium fluid and deposits, and subretinal fluid (SRF) by thresholding the en-face OCT image of the outer retina.

**Materials and Methods:** We retrospectively reviewed medical records of patients with drusen and patients with active central serous chorioretinopathy (CSC). FV number (FVn), average area (FVav), and maximum area (FVmax) and the percentage of nonperfused choriocapillaris area (PNPCA) obtained using the proposed strategy were compared with those obtained by removing only artifacts caused by the superficial capillary plexus (SCP).

**Results:** The SRF group included 21 eyes with active CSC and the drusen group included 29 eyes with nonexudative age-related macular degeneration. FVav, FVmax, FVn, and PNPCA obtained using the algorithm were significantly lower than those obtained by removing only SCP-related artefacts in both groups (all $p<0.05$). The algorithm was also able to remove 96.9% of artifacts secondary to vitreous opacities and all artifacts secondary to serous pigment epithelial detachments.

**Conclusion:** Choriocapillaris nonperfusion areas on OCTA images may be overestimated in eyes with RPE abnormalities and SRF due to artifacts. These artifact areas on choriocapillaris OCTA images can be removed using thresholded images of the outer retina en-face OCT scans. Our new artifact-removal strategy is useful in the assessment of choriocapillaris FV in eyes with SRF, drusen, drusen-like deposits, and pigment epithelial detachment.

**Keywords:** Artifact removal, choriocapillaris flow voids, drusen, optical coherence tomography angiography, subretinal fluid

**Address for Correspondence:** Murat Karaçorlu, İstanbul Retina Institute, İstanbul, Türkiye
E-mail: mkaracorlu@gmail.com **ORCID-ID:** orcid.org/0000-0001-5561-3339
**Received:** 07.01.2022 **Accepted:** 25.04.2022

**Cite this article as:** Ersöz MG, Hocaoğlu M, Sayman Muslubaş I, Arf S, Yıldız E, Karaçorlu M. Artifact-Removed Quantitative Analysis of Choriocapillaris Flow Voids. Turk J Ophthalmol 2023;53:37-43

## Introduction

The choroid is one of the most highly vascularized tissues of the body. Its main function is to supply oxygen and nutrients to the avascular layers of the retina and the retinal pigment pigment epithelium (RPE). The choroid has three vascular layers: Starting from the scleral side, Haller's layer consisting of large-sized vessels, Sattler's layer consisting of medium-sized vessels, and the choriocapillaris. The choriocapillaris is a highly anastomosed, lobular, single-layer network of capillaries. It has a thickness of 10 µm at the fovea and 7 µm at the periphery.[1]

Choroid and choriocapillaris abnormalities play an important role in the pathogenesis of several retinal diseases such as age-related macular degeneration (AMD), central serous chorioretinopathy (CSC), and polypoidal choroidal vasculopathy (PCV).[2,3,4,5,6,7,8,9,10,11,12] Histological studies revealed that the thickness of the choriocapillaris decreases in eyes with AMD and that drusenoid deposits are associated with regions of capillary dropout.[8,10] McLeod et al.[7] reported close association between choriocapillaris degeneration and RPE atrophy in non-exudative AMD with geographic atrophy. They also found that ischemia due to choriocapillaris degeneration stimulates the development of choroidal neovascularization. Studies using indocyanine green angiography revealed the presence of choroidal hyperpermeability and filling defects in eyes with CSC and PCV.[2,9,11] Drusen-like deposits and RPE abnormalities are colocalized with choriocapillaris filling delay and choroid hyperpermeability in eyes with CSC and their fellow eyes.[4,6] Enhanced depth imaging spectral domain optical coherence tomography (SD-OCT) and swept-source OCT revealed that the whole choroid is thickened while the inner choroid is attenuated in eyes with CSC and PCV.[2,3,5,12]

Although abnormalities of the choriocapillaris are involved in the pathogenic mechanisms of common retinal diseases, *in vivo* visualization of the choriocapillaris was not possible until the introduction of OCT-angiography (OCTA). Blood flow appears as bright areas, and flow (signal) void (FV) appears as dark regions in OCTA scans of the choriocapillaris.[13] However, artifacts such as masking, unmasking, motion, projection, and backscattering may cause incorrect signals.[14,15] Regions of masking artifact due to drusen, pigment epithelium detachment (PED), and some RPE lesions can be eliminated,[13] or signal loss secondary to these artifacts can be compensated for with different strategies.[16] However, there has been no appropriate method to overcome all masking and unmasking artifacts due to subretinal fluid (SRF), sub-RPE fluid and deposits, and vitreous opacities.

We performed a new strategy to eliminate artifacts due to fluid or deposit accumulation under RPE, and SRF by using thresholding of outer retina en-face OCT scans. In this study, we aimed to compare choriocapillaris FV measurements obtained using our strategy with those obtained by removing only artifacts caused by the superficial capillary plexus (SCP) in eyes with drusen and eyes with SRF.

## Materials and Methods

We retrospectively reviewed the medical records of 83 patients with non-exudative AMD (drusen group) and 46 patients with active CSC (SRF group) who were referred to our clinic between January 2018 and November 2021 and underwent OCTA imaging. Only one eye of each subject was included. The eyes in both groups had PED and vitreous opacities. The SRF group had also eyes with drusen-like sub-RPE deposits.

Medical history, refractive error measurements, and OCTA images (RTVue-XR Avanti, Optovue, Fremont, CA, USA) were obtained from the patients' medical records. The study protocol was approved by the Institutional Review Board of Şişli Memorial Hospital, İstanbul (approval number: 008, date: 24.12.2021). The study adhered to the tenets of the Declaration of Helsinki.

### OCTA Imaging

En-face OCTA images of the superficial plexus (internal limiting membrane to the inner plexiform layer -10 µm), outer retina (outer border of outer plexiform layer +10 µm to Bruch's membrane -10 µm), and choriocapillaris (Bruch's membrane -10 µm to Bruch's membrane +30 µm) and en-face structural OCT images of the outer retina (outer border of outer plexiform layer +10 µm to Bruch's membrane -10 µm) were obtained using RTVue-XR Avanti with a split-spectrum amplitude-decorrelation angiography algorithm (AngioVue software, version 2017.1.0.151; Optovue Inc.). All images were 6x6 mm and centered on the fovea. The OCTA image of the outer retina was evaluated using the "remove projection" option.

Image Processing

Step 1. En-face OCTA images of the superficial plexus, outer retina, and choriocapillaris and en-face structural OCT images of the outer retina were extracted as .jpg files. Images were then imported into MATLAB (version 9.8.0 [R2020a], MathWorks Inc., Natick, MA, USA). The MATLAB-based stand-alone program and code for analysis are available in https://github.com/erdosty/OCRA/releases/tag/1.46. The images were cropped to remove the markings from the AngioVue software and 5x5 mm images centered on the fovea were used for image analysis. These 5x5 mm images appeared as 500x500 pixels (1 pixel = 10 µm).

Step 2. En-face structural OCT images of the outer retina were used to extract artifacts due to hyperreflective and hyporeflective lesions. On en-face structural OCT images of the outer retina, our MATLAB-based algorithm identified hyperreflective artifacts by Gaussian distribution thresholding and hyporeflective artifacts by maximum entropy thresholding (available at https://github.com/erdosty/OCRA/releases/tag/1.46).[17] Maximum entropy thresholding was applied to OCTA images of the superficial plexus (Figure 1, 2). The thresholded en-face structural OCT images of the outer retina and OCTA image of the superficial plexus were merged to obtain images that included all artifacts (Figure 1-4). Particles function analysis was used to determine the area after exclusion of the artifacts.

Step 3. To determine the global threshold of non-perfusion, the mean of the all pixel values in the en-face OCTA image of the outer retina was calculated. Thresholding was applied to the choriocapillaris image using the global threshold of non-perfusion as previously described (Figure 1).[13] The choriocapillaris pixels under this threshold point were considered non-perfusion.

Step 4. The image including all artifacts and the non-perfusion choriocapillaris image were merged and binarized (Figure 1). Then FV were analyzed using the analyze particles function. The number (FVn), total area, and average area (FVav) of the FV were obtained. The largest FV area (FVmax) was determined by saving "results" as an .xls file and then sorting the areas of FVs. The percentage of non-perfused choriocapillaris area (PNPCA), defined as the percentage of pixels in the choriocapillaris below the non-perfusion global threshold, was calculated using the following formula: PNPCA = (total area of FV/artifact-eliminated analysis area= x 100.[18,19] All of these steps can be performed automatically with the MATLAB-based application of our algorithm (Figure 4).

All steps, except binarization of the en-face structural OCT image of the outer retina, were repeated to obtain an FV image after removing only the artifacts caused by the superficial plexus (Figure 2).

**Exclusion criteria**

Patients whose spherical equivalent refractive error was ≥4.0 diopters were excluded from the study. Any OCTA images with a quality score <8 were excluded from analysis. Patients who had any type of choroidal neovascularization were not included in either groups. Moreover, patients with reticular pseudodrusen were excluded from the drusen group. One of the important points for this image processing method is to know that the Henle fiber layer can appear hyperreflective in OCT images if the retina is scanned with a decentered pupil entry position of the OCT beam.[20] Because of the hyperreflective Henle fiber layer, segmentation errors may occur and healthy tissue may appear more hyperreflective in en-face structural OCT images of the outer retina. Therefore, images scanned with a decentered pupil entry position of the OCT beam were excluded.

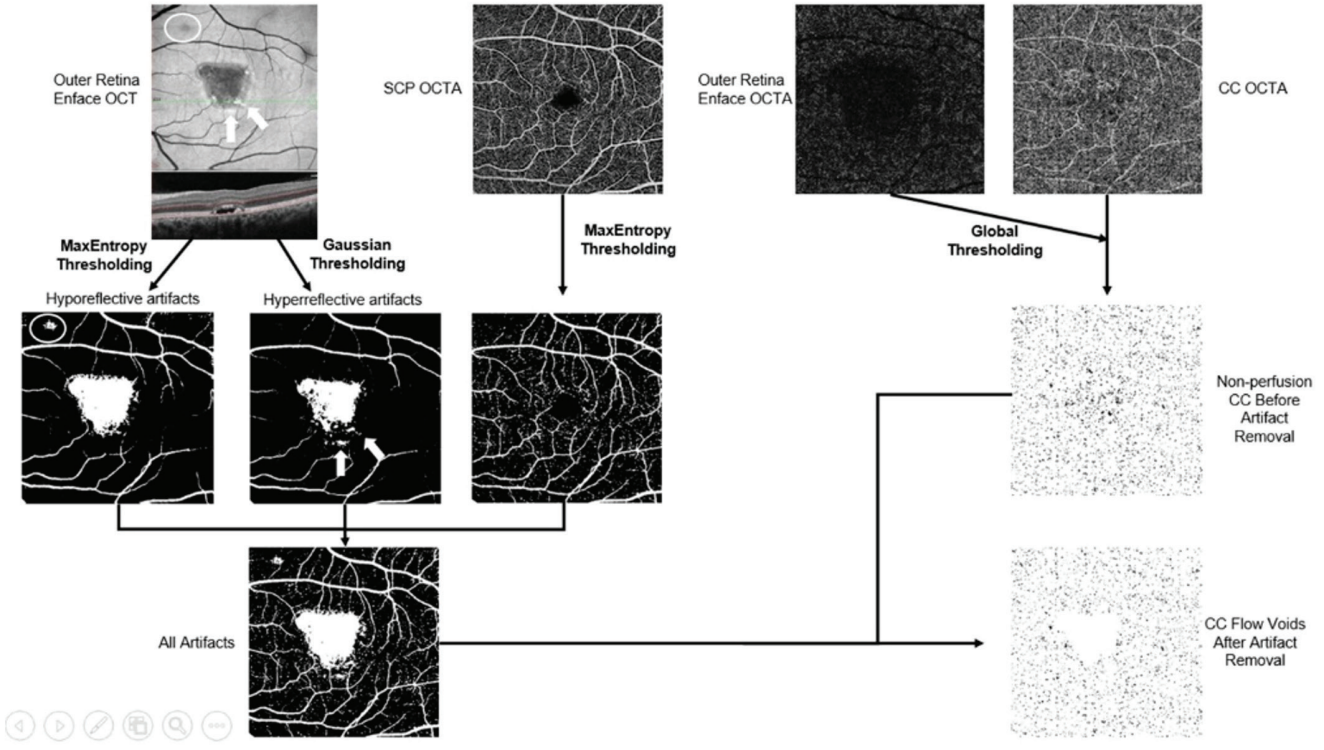


**Figure 1.** Representation of the algorithm used to obtain artifact-removed choriocapillaris (CC) flow voids (FV) in an eye with active acute central serous chorioretinopathy. Before starting image processing, the images were cropped and 5x5 mm images centered on the fovea were imported into MATLAB. For image processing, we first applied two different thresholding algorithms to en-face optical coherence tomography (OCT) images of the outer retina: hyperreflective artifacts were identified by Gaussian distribution thresholding and hyporeflective artifacts by maximum entropy thresholding. Hyporeflective areas due to retinal vessels, subretinal fluid, and vitreous opacities (white circles in the original and thresholded outer retina en-face OCT images) and hyperreflective areas (white arrows in the original and thresholded outer retina en-face OCT images) due to retinal pigment epithelium lesions and dense material accumulation appeared white in these thresholded images. Then we applied maximum entropy thresholding to the OCT angiography (OCTA) image of the superficial capillary plexus (SCP). We merged these three thresholded images (hyporeflective artifacts + hyperreflective artifacts on outer retina en-face OCT + SCP). Then we binarized this combined image and obtained an image in which all artifacts appeared white. To determine the global threshold of non-perfusion, the mean of all pixel values in the outer retina en-face OCTA image was calculated and global thresholding was applied to the CC image using this value. Finally, thresholded images of artifacts and the non-perfusion CC image were merged and binarized to yield an artifact removed CC FV image in which the FV appeared black. Note that the FV co-localized with the artifacts were removed

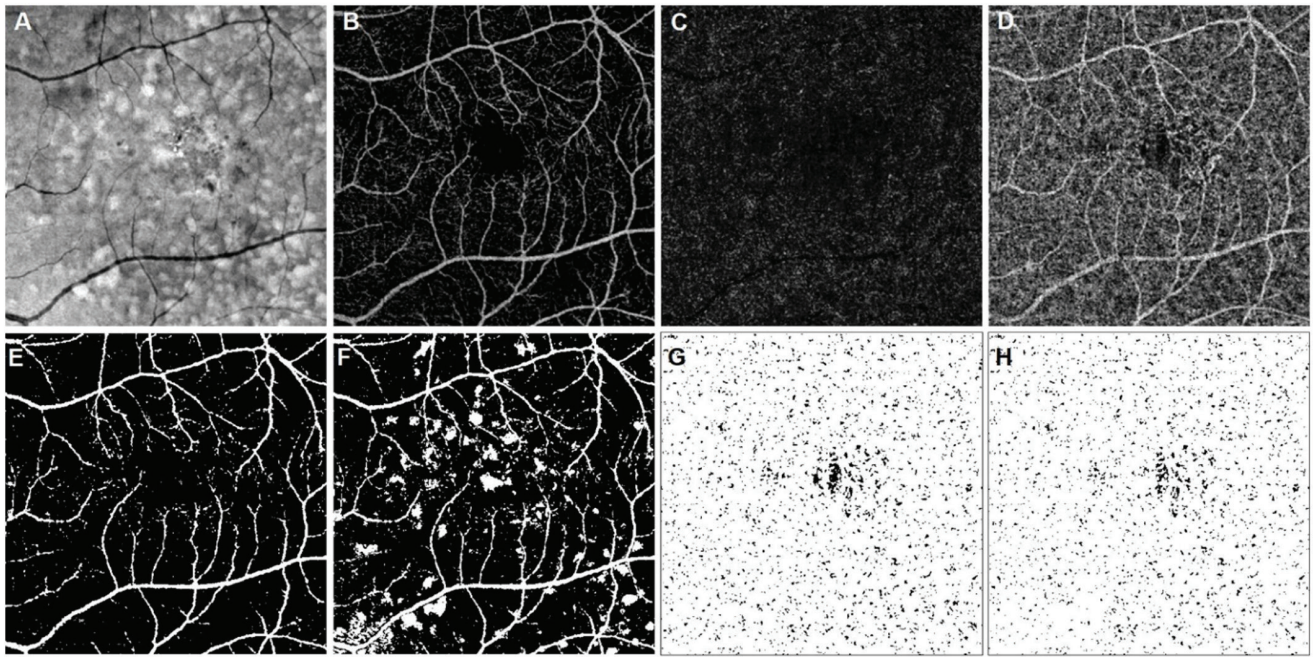


**Figure 2.** Image processing of choriocapillaris (CC) flow void analysis in an eye with drusen. A) En-face structural optical coherence tomography (OCT) image. B) En-face OCT angiography (OCTA) image of the superficial plexus. C) En-face OCTA image of the outer retina. D) En-face OCTA image of the CC. E) Maximum entropy thresholded image of the en-face OCTA image of the superficial plexus. This image also represents the image that contains only the artifacts (white areas) secondary to the superficial plexus. F) The image that includes all artifacts (white areas). G) Flow voids (black areas) after removal of only artifacts caused by the superficial plexus (E). H) Flow voids (black areas) after removal of all artifacts (F)

### Statistical Analysis

All statistical analyses were performed with SPSS (version 21, IBM Corp., Armonk, NY, USA). The Wilcoxon signed ranks test was used to compare FV measurements obtained before and after using our algorithm. $P<0.05$ was considered statistically significant.

## Results

After excluding ineligible patients, the SRF group included 21 eyes with active CSC and the drusen group included 29 eyes with non-exudative AMD. The patients with SRF had a mean age of 45.6±9.4 years (range 35-65 years) and the patients with drusen had a mean age of 69.1±8.5 years old (range 56-83 years). Seven patients (33.3%) in the SRF group and 15 patients (51.7%) in the drusen group were female.

FVn, FVav, FVmax, and PNPCA obtained using our algorithm were significantly lower than those obtained by removing only the SCP in both groups (all; $p<0.05$) (Table 1).

Of the 50 eyes included in our study, 32 had vitreous opacities that caused shadowing artifact. Our algorithm was able to remove these artifacts in 31 eyes (96.9%). In addition, 18 eyes had serous PED and our algorithm removed all serous PEDs causing shadowing of the choriocapillaris.

## Discussion

With OCTA, it is possible to display the SCP, deep capillary plexus, and choriocapillaris separately. Although OCTA provides cross-sectional images, visualization of deep layers, especially the choriocapillaris, is influenced by other tissues and alterations above them. These artifacts may cause overestimation of non-perfused areas of the choriocapillaris.[16,21,22] The commercial software in OCTA devices can remove artifacts secondary to SCP but are unable to remove other artifacts. En-face OCT is very useful to show structural changes in the retina. We used en-face structural OCT images of the outer retina to remove hyperreflective and hyporeflective artifacts because the fovea includes only the outer retinal layers, while en-face OCT images of other layers have relatively higher hyporeflective foveal appearance, which makes these layers unsuitable for image binarization. Moreover, we observed that isoreflective lesions found in the en-face structural OCT images of the outer retina do not lead to masking or unmasking artifacts. As expected, our study revealed that removing hyperreflective and hyporeflective artifacts on en-face structural OCT of the outer retina in addition to artifacts secondary to SCP yielded a lower FVn than was obtained by removing only SCP. We also detected decreses in PNPCA, FVav, and FVmax after using our method in eyes with drusen and SRF.

In eyes with CSC, Aggarwal et al.[21] reported that the shadowing effect of overlying SRF, sub-RPE fluid, and sub-RPE deposits hinders determination of real choriocapillaris FV. Yang et al.[22] found a positive correlation between central subfield thickness and choriocapillaris FV in CSC eyes with SRF due to its shadowing effect and vice versa in CSC eyes without SRF. Many studies have investigated choriocapillaris flow alterations

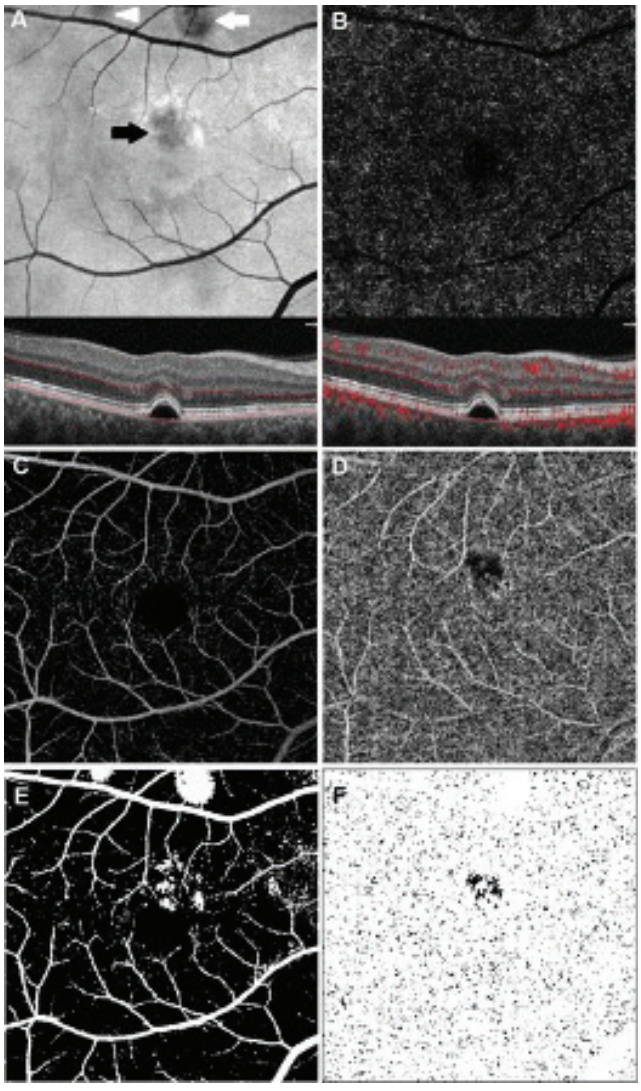


**Figure 3.** Image processing of choriocapillaris (CC) flow void analysis in an eye with subretinal fluid (white arrow), pigment epithelial detachment (black arrow), and vitreous opacity (white arrowhead). A) En-face structural optical coherence tomography (OCT) image and B-scan structural OCT images of the outer retina. B) En-face OCT angiography (OCTA) image and B-scan structural OCT images of the outer retina. C) En-face OCTA image of the superficial plexus. D) En-face OCTA image of the CC. E) The image that includes all artifacts (white areas). Note that the artifacts secondary to subretinal fluid, pigment epithelial detachment, and vitreous opacity appear white. F) Flow voids (black areas) after removal of all artifacts

in eyes with CSC but none of them has overcome OCTA visualization artifacts.[15,21,22,23,24,25,26]

Several studies have been conducted in patients with AMD to obtain choriocapillaris images with drusen artifacts removed.[13,16,18,19] Borrelli et al.[18] used binarized RPE elevation images to eliminate areas with drusen. However, using this method causes exclusion of all RPE lesions and some of these lesions do not lead to artifacts. Nesper et al.[13] obtained drusen-artifact-removed choriocapillaris images with binarized en-face structural OCT images of the RPE layer. Only hyporeflective artifacts in en-face structural OCT can be removed by using their method, but most of the RPE lesions cause hyperreflective artifacts in en-face structural OCT of the RPE or outer retina. Using an RPE elevation map, Zhang et al.[16] managed to compensate for signal reduction secondary to drusen without excluding any area. They reported a decrease in FV after signal compensation. However, artifacts due to very dense and shallow lesions can not be compensated for as much as artifacts due to light and elevated lesions, because their method considered the height but not density of RPE alterations. Their method can overcome artifacts due to sub-RPE fluid but not those due to SRF and vitreous opacities. Recently, Hwang et al.[27] used a modified version of Zhang et al's[16] method in eyes with active CSC in an attempt to compensate for artifacts secondary to SRF. However, as they noted in their study, the compensated images did not differ significantly from the original image.[27] To the best of our knowledge, none of the previous automated methods can eliminate or compensate for all artifacts due to SRF, PED, hyperreflective RPE lesions, and vitreous opacities. We have overcome these artifacts by removing hyperreflective and hyporeflective artifacts on en-face structural OCT of the outer retina and keeping the isoreflective lesion areas that do not cause artifacts. We applied global thresholding to reveal non-perfusion areas in the choriocapillaris (step 3). Other thresholding methods, such as Phansalkar thresholding, can also be used with our artifact removal process instead of step 3. In a very recent report, Burnasheva et al.[28] manually removed hyporeflective and hyporeflective artifacts by using the en-face structural OCT image of the whole retinal slab to evaluate FV in eyes with CSC. However, healthy areas and artifacts are separated more clearly using en-face structural OCT images of the outer retina than of the whole retinal slab. Moreover, using an automated method avoids user-dependent bias.

### Study Limitations

This study only focused on the effect of artifact removal on FV parameters in eyes with RPE abnormalities and SRF. Further studies are required for investigating FV alterations in specific retinal diseases.

## Conclusion

Non-perfusion areas in the choriocapillaris may be overestimated in eyes with RPE abnormalities and SRF. These areas can be removed using thresholded images of outer retina en-face OCT scans. Our new artifact-removal strategy is useful in the assessment of choriocapillaris FV in eyes with SRF, drusen, drusen-like deposits, and sub-RPE fluid. Artifacts secondary to vitreous opacities can also be removed with our strategy.

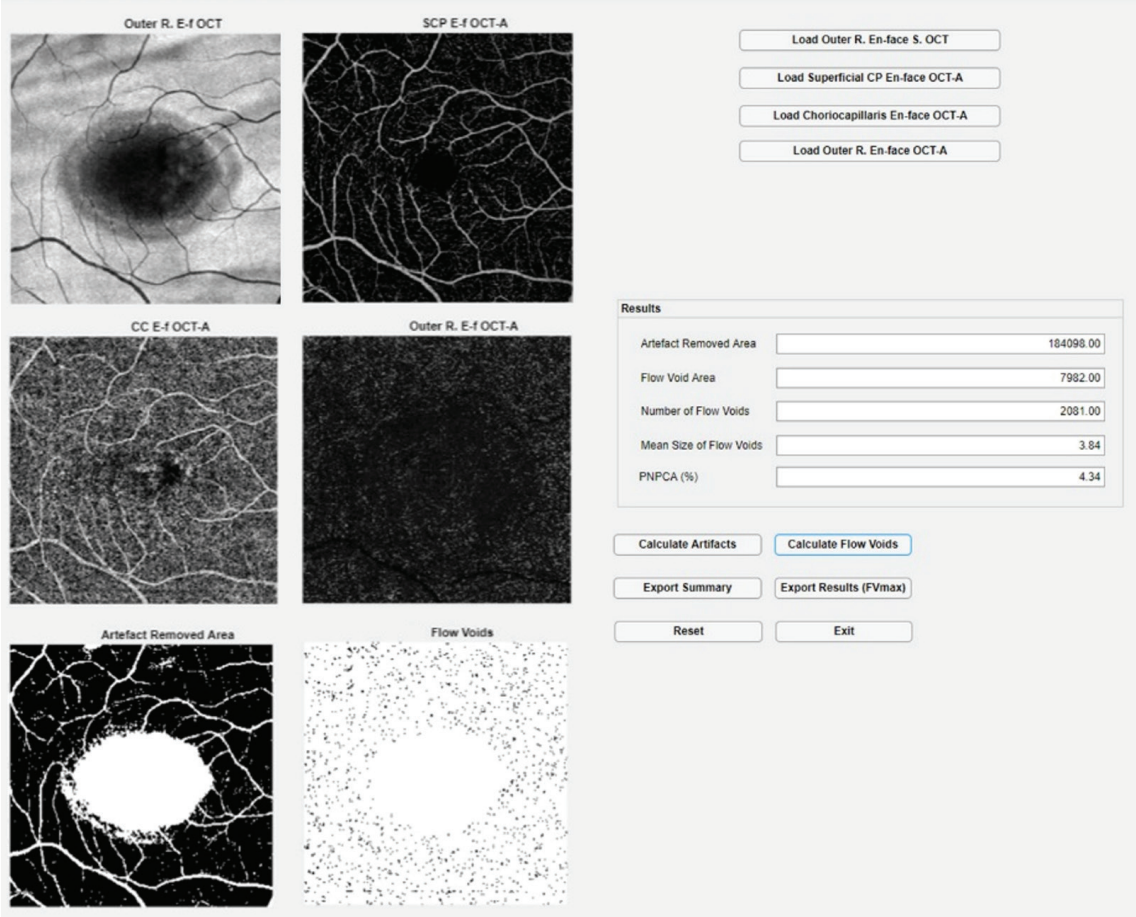


**Figure 4.** Automated image processing with our strategy using a MATLAB-based application in an eye with subretinal fluid. The user loads the en-face structural optical coherence tomography (OCT) image of the outer retina, superficial capillary plexus (SCP) OCT-angiography (OCTA) image, choriocapillaris OCTA image, and outer retina OCTA image. The "calculate artifacts" option generates an "artifact-removed area" image in which artifacts appear white. It also calculates the artifact-removed area in pixels (1 pixel = 10 µm, 1 pixel$^2$ = 100 µm$^2$). The "calculate flow voids" option generates a "flow voids (artifact removed)" image and also calculates flow void area, number, and average size, and the percentage of non-perfused choriocapillaris area (PNPCA). The maximum size of flow void areas can be obtained using the "export results (FVmax)" option

**Table 1. Comparison of choriocapillaris flow voids and non-perfused area obtained using the present algorithm vs. obtained by removing only the superficial capillary plexus**

| | **Subretinal Fluid** | | | **Drusen** | | |
|---|---|---|---|---|---|---|
| **Parameter** | **Only SCP removed (n=21)** | **Present algorithm, (n=21)** | **p** | **Only SCP removed, (n=29)** | **Present algorithm, (n=29)** | **p** |
| PNPCA (mean) | 6.1±1.8 | 5.8±1.8 | <0.001 | 7.4±3.2 | 6.9±2.9 | <0.001 |
| Choriocapillaris FV | | | | | | |
| FVn (n), (mean) | 2807.7±385.2 | 2639.4±390 | <0.001 | 2542.8±328.5 | 2444.6±332.8 | <0.001 |
| FVav (µm$^2$), (mean) | 476±97.6 | 439.6±83.8 | <0.001 | 637.7±235.8 | 581.7±205.6 | <0.001 |
| FVmax (µm$^2$), (mean) | 37938.1±80997.3 | 10266.7±10993.7 | 0.001 | 77289.9±157329.4 | 60727±127921.8 | 0.001 |

SCP: Superficial capillary plexus, FVav: Average area of flow void, FVmax: Maximum area of flow void, FVn: Number of flow voids, PNPCA: Percentage of non-perfused area in the choriocapillaris

**Ethics**

**Ethics Committee Approval:** The study protocol was approved by the Institutional Review Board of Şişli Memorial Hospital, İstanbul (approval number: 008, date: 24.12.2021).

**Informed Consent:** Retrospective study.

**Peer-review:** Externally and internally peer-reviewed.

**Authorship Contributions**

Surgical and Medical Practices: M.K., S.A., M.G.E., M.H., I.S.M., Concept: M.K., S.A., M.G.E., Design: M.K., M.G.E, E.Y., Data Collection or Processing: M.G.E., E.Y., Analysis or

Interpretation: M.K., M.G.E., Literature Search: M.G.E., M.H., I.S.M., Writing: M.G.E., M.K., S.A.

**Conflict of Interest:** No conflict of interest was declared by the authors.

**Financial Disclosure:** The authors declared that this study received no financial support.

## References


1. Nickla DL, Wallman J. The multifunctional choroid. Prog Retin Eye Res. 2010;29:144-168.
2. Cheung CMG, Lee WK, Koizumi H, Dansingani K, Lai TYY, Freund KB. Pachychoroid disease. Eye (Lond). 2019;33:14-33.
3. Chung SE, Kang SW, Lee JH, Kim YT. Choroidal thickness in polypoidal choroidal vasculopathy and exudative age-related macular degeneration. Ophthalmology. 2011;118:840-845.
4. Ersoz MG, Arf S, Hocaoglu M, Sayman Muslubas I, Karacorlu M. Indocyanine Green Angiography of Pachychoroid Pigment Epitheliopathy. Retina. 2018;38:1668-1674.
5. Imamura Y, Fujiwara T, Margolis R, Spaide RF. Enhanced depth imaging optical coherence tomography of the choroid in central serous chorioretinopathy. Retina. 2009;29:1469-1473.
6. Matsumoto H, Mukai R, Morimoto M, Tokui S, Kishi S, Akiyama H. Clinical characteristics of pachydrusen in central serous chorioretinopathy. Graefes Arch Clin Exp Ophthalmol. 2019;257:1127-1132.
7. McLeod DS, Grebe R, Bhutto I, Merges C, Baba T, Lutty GA. Relationship between RPE and choriocapillaris in age-related macular degeneration. Invest Ophthalmol Vis Sci. 2009;50:4982-4991.
8. McLeod DS, Lutty GA. High-resolution histologic analysis of the human choroidal vasculature. Invest Ophthalmol Vis Sci. 1994;35:3799-3811.
9. Prünte C, Flammer J. Choroidal capillary and venous congestion in central serous chorioretinopathy. Am J Ophthalmol. 1996;121:26-34.
10. Ramrattan RS, van der Schaft TL, Mooy CM, de Bruijn WC, Mulder PG, de Jong PT. Morphometric analysis of Bruch's membrane, the choriocapillaris, and the choroid in aging. Invest Ophthalmol Vis Sci. 1994;35:2857-2864.
11. Sasahara M, Tsujikawa A, Musashi K, Gotoh N, Otani A, Mandai M, Yoshimura N. Polypoidal choroidal vasculopathy with choroidal vascular hyperpermeability. Am J Ophthalmol. 2006;142:601-607.
12. Warrow DJ, Hoang QV, Freund KB. Pachychoroid pigment epitheliopathy. Retina. 2013;33:1659-1672.
13. Nesper PL, Soetikno BT, Fawzi AA. Choriocapillaris Nonperfusion is Associated With Poor Visual Acuity in Eyes With Reticular Pseudodrusen. Am J Ophthalmol. 2017;174:42-55.
14. Chen FK, Viljoen RD, Bukowska DM. Classification of image artefacts in optical coherence tomography angiography of the choroid in macular diseases. Clin Exp Ophthalmol. 2016;44:388-399.
15. Matet A, Daruich A, Hardy S, Behar-Cohen F. Patterns Of Choriocapillaris Flow Signal Voids In Central Serous Chorioretinopathy: An Optical Coherence Tomography Angiography Study. Retina. 2019;39:2178-2188.
16. Zhang Q, Zheng F, Motulsky EH, Gregori G, Chu Z, Chen CL, Li C, de Sisternes L, Durbin M, Rosenfeld PJ, Wang RK. A Novel Strategy for Quantifying Choriocapillaris Flow Voids Using Swept-Source OCT Angiography. Invest Ophthalmol Vis Sci. 2018;59:203-211.
17. Gargouri F. Thresholding the Maximum Entropy. MATLAB Central File Exchange. Vol 2020. https://www.mathworks.com/matlabcentral/fileexchange/35158-thresholding-the-maximum-entropy2020.
18. Borrelli E, Souied EH, Freund KB, Querques G, Miere A, Gal-Or O, Sacconi R, Sadda SR, Sarraf D. Reduced Choriocapillaris Flow in Eyes with Type 3 Neovascularization and Age-Related Macular Degeneration. Retina. 2018;38:1968-1976.
19. Borrelli E, Uji A, Sarraf D, Sadda SR. Alterations in the Choriocapillaris in Intermediate Age-Related Macular Degeneration. Invest Ophthalmol Vis Sci. 2017;58:4792-4798.
20. Staurenghi G, Sadda S, Chakravarthy U, Spaide RF; International Nomenclature for Optical Coherence Tomography (IN•OCT) Panel. Proposed lexicon for anatomic landmarks in normal posterior segment spectral-domain optical coherence tomography: the IN•OCT consensus. Ophthalmology. 2014;121:1572-1578.
21. Aggarwal K, Agarwal A, Deokar A, Mahajan S, Singh R, Bansal R, Sharma A, Dogra MR, Gupta V; OCTA Study Group. Distinguishing features of acute Vogt-Koyanagi-Harada disease and acute central serous chorioretinopathy on optical coherence tomography angiography and en face optical coherence tomography imaging. J Ophthalmic Inflamm Infect. 2017;7:3.
22. Yang HS, Kang TG, Park H, Heo JS, Park J, Lee KS, Choi S. Quantitative evaluation of choriocapillaris using optical coherence tomography and optical coherence tomography angiography in patients with central serous chorioretinopathy after half-dose photodynamic therapy. PLoS One. 2020;15:e0227718.
23. Cakir B, Reich M, Lang S, Bühler A, Ehlken C, Grundel B, Stech M, Reichl S, Stahl A, Böhringer D, Agostini H, Lange C. OCT Angiography of the Choriocapillaris in Central Serous Chorioretinopathy: A Quantitative Subgroup Analysis. Ophthalmol Ther. 2019;8:75-86.
24. Gal-Or O, Dansingani KK, Sebrow D, Dolz-Marco R, Freund KB. Inner choroidal flow signal attenuation in pachychoroid disease: Optical Coherence Tomography Angiography. Retina. 2018;38:1984-1992.
25. Rochepeau C, Kodjikian L, Garcia MA, Coulon C, Burillon C, Denis P, Delaunay B, Mathis T. Optical Coherence Tomography Angiography Quantitative Assessment of Choriocapillaris Blood Flow in Central Serous Chorioretinopathy. Am J Ophthalmol. 2018;194:26-34.
26. Demirel S, Özcan G, Yanık Ö, Batıoğlu F, Özmert E. Vascular and structural alterations of the choroid evaluated by optical coherence tomography angiography and optical coherence tomography after half-fluence photodynamic therapy in chronic central serous chorioretinopathy. Graefes Arch Clin Exp Ophthalmol. 2019;257:905-912.
27. Hwang BE, Kwak JH, Kim JY, Kim RY, Kim M, Park YG, Park YH. Quantitative analysis of choroidal blood flow parameters in optical coherence tomography and angiography in central serous chorioretinopathy. Graefes Arch Clin Exp Ophthalmol. 2022;260:2111-2120.
28. Burnasheva MA, Kulikov AN, Maltsev DS. Artifact-Free Evaluation of Choriocapillaris Perfusion in Central Serous Chorioretinopathy. Vision (Basel). 2020;5:3.